Hard X-ray polarimetry with Astrosat-CZTI

S. V. Vadawale[1], T. Chattopadhyay[1,2], A. R. Rao[3], D. Bhattacharya[4], V. B. Bhalerao[4], N. Vagshette[4], P. Pawar[5], and S. Sreekumar[6]

[1] Physical Research Laboratory, Navarangpura, Ahmedabad 380009, India
[2] Indian Institute of Technology Gandhinagar, Ahmedabad 382424, India
[3] Tata Institute of Fundamental Research, Homi Bhabha Road, Colaba, Mumbai 400005, India
[4] Inter-University Centre for Astronomy and Astrophysics, Post Bag 4, Pune 411007, India
[5] Swami Ramanand Teerth Marathwada University, Nanded 431604, India
[6] Vikram Sarabhai Space Centre, VRC, Thiruvananthapuram 695022, India

Received Date / Accepted Date

ABSTRACT

X-ray polarimetry is largely an unexplored area of an otherwise mature field of X-ray astronomy. Except for a few early attempts during 1970s, no dedicated X-ray polarimeter has been flown during the last four decades. On the other hand, the scientific value of X-ray polarization measurement is well known for a long time and there has been significant technical progress in developing sensitive X-ray polarimeters in the recent years. But there are no approved dedicated X-ray polarimetric experiments to be flown in the near future and hence it is important to explore the polarimetric capabilities of other existing or planned instruments and examine whether they can provide significant astrophysical polarization measurements. In this paper, we present experimental results to show that the CZTI instrument onboard the forthcoming Indian astronomy mission, Astrosat, will be able to provide sensitive measurements of X-ray polarization in the energy range of 100 - 300 keV. CZTI will be able to constrain any intrinsic polarization greater than $\sim 40\%$ for bright X-ray sources (>500 mCrab) within a short exposure of $\sim$100 ks with a 3 sigma confidence level. We show that this seemingly 'modest' sensitivity can play a very significant role in addressing long pending questions like the contribution of relativistic jets to hard X-rays in black hole binaries and X-ray emission mechanism and geometry in X-ray pulsars.

Key words. Instrumentation: polarimeters — X-rays: individual (Cygnus X-1, Crab) — techniques: polarimetric

1. Introduction

Polarization is a very important property of radiation from astrophysical sources and it carries unique information regarding the emission mechanism, physical conditions as well as emission geometry at the source. The importance of polarization measurement was realized from the very early days of X-ray astronomy (Novick 1975; Meszaros et al. 1988; Kallman 2004; Krawczynski et al. 2011, and references therein) and there exists a large body of theoretically expected polarization signatures from different types of X-ray sources. However, despite the tremendous progress in other fields of X-ray astronomy, the field of X-ray polarimetry has been largely unexplored observationally (Weisskopf 2010). The primary reason for this is the extremely photon hungry nature of polarimetry (Weisskopf et al. 2010; Elsner et al. 2012), which along with the low efficiency and other technical difficulties of different polarization measurement methods result in a poor sensitivity for a dedicated polarimetric mission compared to the traditional spectroscopic, timing or imaging missions of comparable size and cost. Consequently there is no dedicated X-ray polarimetry mission approved, *despite having many proposed missions as well as balloon born experiments (McConnell et al. 2009; Costa et al. 2010; Tagliaferri et al. 2010; Pearce et al. 2012; Soffitta et al. 2013; Guo et al. 2013; Kislat et al. 2013; Dong 2014), some of them being considered at an advanced stage of selection (Paul et al. 2010).* On the other hand, there is a growing realisation in recent times that due to the improved techniques of polarisation a dedicated polarimetry mission would provide quite fresh results. *A dedicated X-ray polarimetry mission GEMS (Jahoda 2010) was selected for development as part of the NASA Small Explorer program in 2009, but was discontinued in 2012 due to programatic reasons. It has been proposed again at the 2014 SMEX NASA call, which has also attracted two more proposals dedicated to X-ray polarimetry, indicating enhanced interest of community in having firm X-ray polarization measurements.* Still, in the absence of any approved dedicated mission, it is very important to explore any possibility of obtaining meaningful X-ray polarization measurements from instruments designed for other related purposes (like X-ray timing and spectroscopy) and to have a robust ground calibration.

There have been many attempts to retrieve polarimetric information from the existing X-ray instruments having notional polarimetric sensitivity, the noted results being measurement of highly polarized emission from a GRB with the RHESSI mission and from two Galactic X-ray sources (Cygnus X-1, a black hole binary and Crab, a pulsar wind nebula) with the IBIS and the SPI instruments onboard the Integral mission (Coburn & Boggs 2003; Forot et al. 2008; Laurent et al. 2011; Jourdain et al. 2012). These measurements, however, faced some criticisms because these instru-

ments are not fully optimized for polarimetry and particularly because their polarimetric capabilities were not calibrated before launch (Rutledge & Fox 2004; Zdziarski et al. 2014).

Here we experimentally show that the Cadmium-Zinc-Telluride Imager (CZTI) on board the forthcoming Indian astronomy mission Astrosat will be capable of measuring polarization of the incident X-rays in the energy range 100 - 300 keV. In the next section we discusses basic concepts of X-ray polarimetry with CZTI which is followed by discussion on the experiment and the results demonstrating the polarimetric capability of CZTI. Following this we discuss the overall polarimetric sensitivity of CZTI with realistic polarimetric background in Section 4 and the astrophysical significance of the polarimetric capability of CZTI in Section 5 before concluding in Section 6.

2. X-ray polarimetry with Astrosat-CZTI

Astrosat is an Indian multi-wavelength astronomy mission scheduled to be launched in late 2015. It consists of five instruments covering a range of spectrum from optical to hard X-rays (Singh et al. 2014; Agrawal 2006). The Cadmium-Zinc-Telluride Imager (CZTI) on board Astrosat, which is primarily designed for hard X-ray imaging and spectroscopy, is one instrument expected to be sensitive to polarization of the incident X-rays due to its large pixilated detector plane. The CZTI is a coded aperture mask telescope with a total active area of 1024 cm^2. The detector plane consists of 64 detector modules arranged in four identical quadrants, each having 16 modules arranged in a square geometry. Each module is an independent CZT (Cadmium-Zinc-Telluride) detector with a $16{\times}16$ array of pixels, each of size 2.5 mm${\times}$2.5 mm. The 5 mm detector thickness provides detection efficiency at energies higher than the primary spectroscopic energy range of 10 - 100 keV, where significant fraction of photons interaction is by means of Compton scattering. In such events, the Compton scattered photon could be detected in an adjacent pixel. Since the direction of the scattered photon depends on the polarization direction of the incident photon, such pixelated detectors can in general, and Astrosat-CZTI in particular, be used as a Compton X-ray polarimeter (Chattopadhyay et al. 2014, hereafter C14). In the energy range of interest for CZTI i.e. $100-300$ keV, the energy of the recoil electron is much smaller than the energy of the scattered photon. Hence it is assumed that the pixel with the lower energy deposition is the scattering pixel and the second pixel is the absorbing pixel. Another important criterion determined by C14 to select the valid double pixel events is to require that the ratio of energies deposited in two adjacent pixels be greater than 2. The azimuthal angle of the Compton scattering is determined from the direction of the centre of the scattering pixel to the centre of the absorbing pixel with reference to a pre-defined instrument reference plane. Histogram of the azimuthal scattering angles over 8 angular bins, corresponding to the four edge pixels and the four corner pixels can be used to quantify the scattering modulation. It should be noted that this histogram has an inherent modulation due to unequal angular bins corresponding to the edge and the corner pixels, respectively. However, this inherent modulation pattern can be corrected by normalizing the measured azimuthal distribution with

the azimuthal distribution for unpolarized beam (Lei et al. 1997; Krawczynski et al. 2011).

If $N_{i,pol}$ is the number of counts in the ith bin for 100 % polarized beam and $M_{i,unpol}$ is the counts in that bin for 100 % unpolarized beam and $\bar{M}_{unpol}$ is mean counts, then normalised counts in the ith bin are given by

$$N_{i,cor} = \frac{N_{i,pol}}{M_{i,unpol}} \bar{M}_{unpol} \qquad (1)$$

The corrected azimuthal modulation pattern, the so called modulation curve, can then be fitted by

$$C(\phi) = A\cos^2(\phi - \phi_0) + B \qquad (2)$$

and the modulation amplitude is then defined by

$$\mu = \frac{A}{A + 2B} \qquad (3)$$

Figure 1 shows the corrected and uncorrected modulation curves for three different polarization angles with reference to the pixel edge. It can be seen that the modulation factors, obtained by fitting eq. 2 to the corrected modulation curves are different for different polarization angles. This results in different polarization sensitivity at different polarization angles as discussed in C14 (also see Section 4).

The sensitivity of an X-ray polarimeter is specified in terms of MDP (Minimum Detectable Polarization) given by,

$$MDP_{99\%} = \frac{4.29}{\mu_{100}R_{src}} \sqrt{\frac{R_{src} + R_{bkg}}{T}} \qquad (4)$$

where R_{src} and R_{bkg} are the source and background count rates. T is the exposure time and μ_{100}, *the so called the modulation factor, is the modulation amplitude for for 100% polarized beam.*

Based on extensive simulations, we had shown in C14 that the Astrosat-CZTI will have significant polarization measruement capabilities in the energy range of $100 - 300$ keV, particulalry for bright (> 500 mCrab) X-ray sources.

3. Experimental confirmation

In order to confirm the polarimetric capability of CZTI, we carried out an X-ray polarization measurement experiment using the actual flight model of CZTI module ensuring that all properties of flight electronics are also included in the experiment. We produced a partially polarized beam of X-rays by scattering 356 keV X-rays from the radio-active source ^{133}Ba at $\sim$90 degrees (see figure 2). A 6 cm long Aluminium cylinder was used as a scatterer. The source and the scatterer were placed inside a 4 cm thick Lead cylinder with a slit of 5 cm length and 2 mm width. The CZTI module is kept below the slit such that only the photons from ^{133}Ba scattered at 90° by the Aluminium scatterer can reach the CZTI detector. With this setup, the angle of scattering is constrained to 90°±15° implying a partially polarized beam of energy between 190 keV and 240 keV.

The basic data filtering and analysis were carried out as discussed in C14. This involved selection of appropriate adjacent double pixel events, generating 8 bin azimuthal
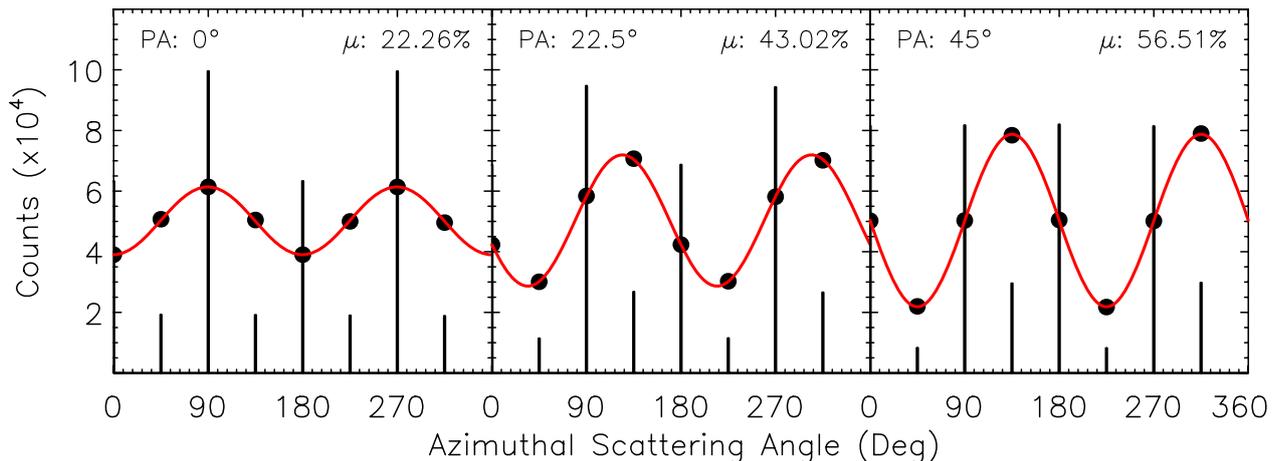
Fig. 1. Simulated histograms of azimuthal scattering angles for three polarization angles $0°$, $22.5°$ and $45°$ with reference to the pixel edge for 100% polarized beam. The vertical lines show uncorrected histograms showing effect of unequal angular bins. Black dots show corrected values for each bin (see equation 1) and the red lines represents fit (equation 2) to these points.
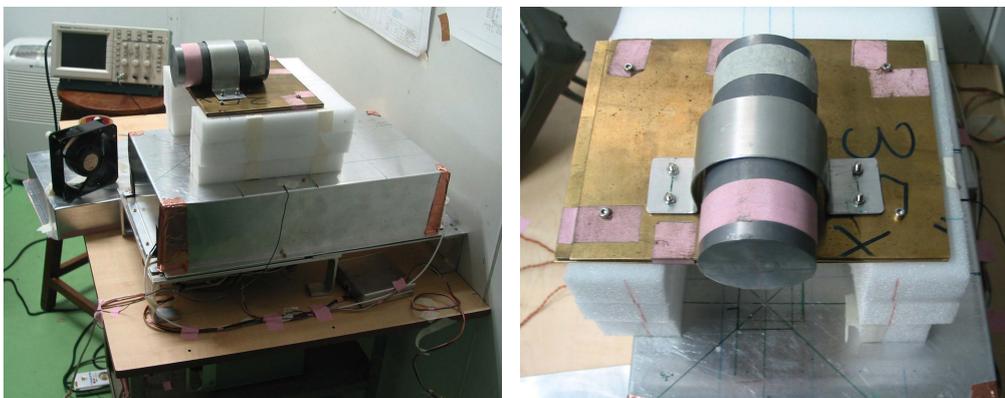

Fig. 2. Left: Polarization experiment setup with CZTI. Right: zoomed view of the setup

distribution with reference to lower energy pixel and correcting azimuthal distribution for the unequal angle bins. Figure 3 shows the corrected modulation curves for partially polarized beam at two different polarization angles, $0°$ and $45°$, with reference to one of the edges of the CZT detector module as well as for an unpolarized beam (direct exposure to 356 keV X-rays). It can be seen that the modulation curves for the measurements at these polarization angles show clear signature of the polarization of the incident beam and the *modulation curves corresponding to different* polarization angles also change as expected. The errors in the observed modulations are nominal 1σ errors and the simulation results too have errors of similar magnitudes. In the case of the unpolarized beam, the residual modulation, which could be due to the instrumental artifacts, is almost neglible (1 %) and thus will not have any significant effect on the polarization measurement aimed at largely polarized source. It should be noted here that one major criticism of the recent X-ray polarization measurements by INTEGRAL IBIS and SPI instruments is that these instruments were never tested with an unpolarized beam.

These results clearly demonstrate that CZTI is capable of detecting polarization of the incident X-rays. *However, the observed modulation amplitude cannot be directly used to validate the simulation because of the partially polarized beam.* In order to have a quantitative comparison with the simulations, we repeated the simulations for the exact geometry of the experiment including the generation of the polarized beam and considered the experimentally measured background to calculate the modulation factor. The modulation factors obtained from these simulations typically agree within $\sim$1 % of the experimentally measured modulation factors, in all the cases. This implies that the value of μ_{100} obtained from simulations do represent realistic modulation factor.

4. Polarimetric Background and Sensitivity

The confidence provided by the experimental verification of the polarization measurement capability of CZTI enables us to use the simulation methods to quantify the actual polarimetric sensitivity of CZTI in the astrophysical context. In the case of CZTI, the sensitivity is determined by the polarimetric background, R_{bkg}, because the background
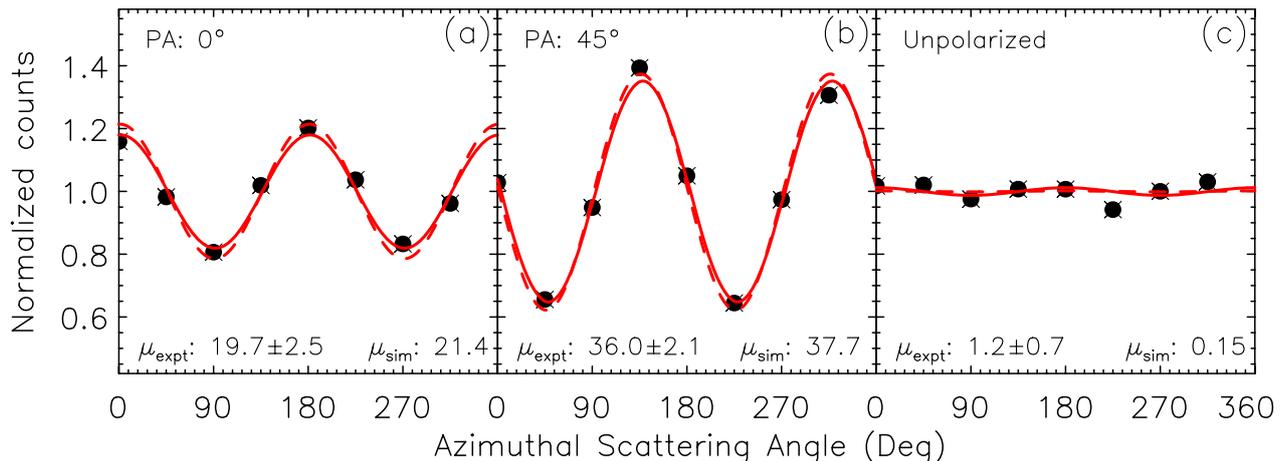
Fig. 3. (a) and (b) Experimentally measured modulation curves for partially polarized X-rays from ^{133}Ba source at two polarization angles $0°$, and $45°$ respectively. (c) The same curve measured for unpolarized X-rays from ^{133}Ba. The dashed line shows the modulation curves obtained from the Geant4 simulations of the experimental setup.

is primarily dominated by the Compton scattering of the diffuse X-ray background as shown in C14 and can be as high as the source count rate. This is because the primary spectroscopic energy range for the CZTI is up to 100 keV whereas the polarization measurements are possible only at energies > 100 keV due to the requirement of detecting the primary scattering event. Hence the coded mask as well as the shielding and other support structure gets increasingly transparent in the polarimetric energy range of CZTI. The large polarimetric background also results in degradation of the modulation curve. Therefore, to determine the unknown degree of polarization of the incident X-rays, the actual modulation factor, μ_{100} has to be replaced by degraded modulation factor, $\mu_{d,100}$. Both these aspects were considered in detail in C14 and it was found that CZTI will have significant polarimetric capabilities despite having semi-transparent shielding. The total polarimetric background (i.e. total double pixel events passing all the filtering criteria) was almost the same as the total polarimetric count rate from Crab. It was pointed out to us (E. Costa, private communication) that calculations of C14 did not include background due to the Earth's X-ray albedo which is now included in our revised calculations (we assume that the albedo background is not polarized which is a fair assumption becuase of the low earth orbit of Astrosat and resultant azimuthal symmetry in scattering of albedo from the Earth's atmosphere) Also we have significantly improved our calculations to include effective shielding at individual detector module level. This enables us to calculate module wise polarimetric background as shown in Figure 4 and thus provide more reliable estimate of effective background.

The estimated effective background is now ~1.5 Crab and hence the expected polarimetric sensitivity, as shown in Figure 5 in terms of MDP as a function of source intensity, is slightly less than that presented in C14. One important repercussion of our module-wise background calculation is the realization that different subsets of CZTI detector plane will have different sensitivities according to the net back-

ground for the given subset. This provides a very powerful handle to cross-verify the actual polarization measurement between different subsets and thus to have enhanced confidence in the polarization measurement. It should be noted here that due to the availability of event wise data, all such sub sampling, either in selection of module subset or the energy range can be carried out at the analysis level and thus does not impose any special restriction on the actual observation.

Figure 5 shows the polarimetric sensitivity of CZTI in terms of MDP as a function of source intensity. It can be seen that for a Crab like source, MDP of 5 % can be achieved in exposure time of ~1 Ms (million seconds). Though such long exposure times are routinely quoted in the context of X-ray polarimetry, these may not be realistic for the observatory class mission such as Astrosat. On the other hand, in the energy range of interest $(100 − 300$ keV) the emission from almost all X-ray sources is expected to be of non-thermal origin and thus can be highly polarized. This is corroborated by the recent reports of more then 50 % polarized soft gamma emission by Integral from two bright X-ray sources Crab and Cygnus X-1 (Forot et al. 2008; Laurent et al. 2011; Jourdain et al. 2012). In this context a more appropriate question is - given highly polarized X-ray emission, how well its polarization can be constrained by CZTI with a typical exposure time of few tens of kilo-seconds.

For an unknown source, the polarization degree P is given by -

$$P = \frac{\mu}{\mu_{d,100}} \qquad (5)$$

where, μ and $\mu_{d,100}$ are the measured modulation amplitude for that source and the degraded modulation factor respectively. It should be noted that the degraded modulation factor $\mu_{d,100}$ takes into account the effect of Compton scattering of the background photons (both cosmic X-ray background as well as albedo background) as discussed in C14 and hence it is smaller then μ_{100} obtained from Geant4
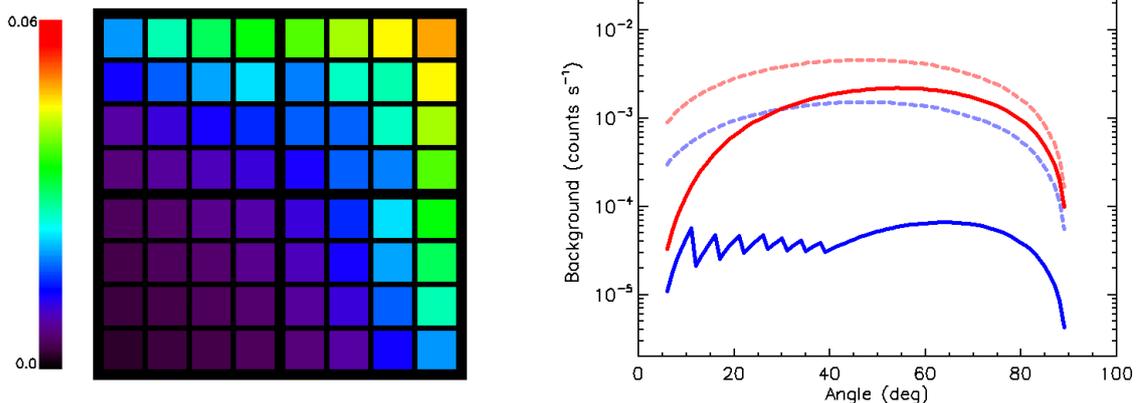
Fig. 4. left: Polarimetric background in the energy range of 100 − 300 keV expected for individual detector modules of CZTI. right: Angle dependent contribution of diffuse X-ray background to the total background for the innermost (blue) and outer most module (red) to demonstrate the effect of collimators and module location. The dashed curves show background without considering module wise collimators.

simulations. Error in the measurement is given by

$$\frac{\sigma_P}{P} = \sqrt{\frac{\sigma_\mu^2}{\mu^2} + \frac{\sigma_{\mu_{d,100}}^2}{\mu_{d,100}^2}} \qquad (6)$$

where, σ_μ is the statistical error associated with the measurement of modulation factor μ which depends on both the degree of polarization in the source and the source intensity. $\sigma_{\mu_{d,100}}$ is the error in $\mu_{d,100}$.

It should be noted that $\sigma_{\mu_{d,100}}$ depends on the relative angle between the polarization direction of the incident X-rays and a reference direction of the instrument. In general, the polarization angle can not be constrained to better than $28.5°/(P/\sigma_P)$ simply by fitting the modulation curves (Strohmayer & Kallman 2013). Thus in most cases, the uncertainty in polarization angle can be assumed to be $15° - 20°$. Figure 5 shows the detection significance for different source intensities as a function of exposure time, with $\mu_{d,100}$ and $\sigma_{\mu_{d,100}}$ corresponding to the average polarization angle of $22.5°$ and uncertainty in polarization angle of $\pm10°$. It can be seen that for large exposure times, the significance of polarization measurement saturates due to the uncertainty in $\mu_{d,100}$. However, for smaller exposure times (100 ks), the uncertainty in polarization measurement is dominated by the counting statistics. Since the large exposure times are expected to be resulting from multiple smaller exposure times with different position angle of the spacecraft, it is more appropriate to consider the average polarization angle of $22.5°$ (this is the angle with reference to the instrument reference direction and not the absolute polarization angle in the sky frame). However, in many such cases, it might be possible to have better constrains on absolute polarization angle based on multiple smaller subset of the same data, which may result in higher significance of the polarization measurement. Another factor affecting detection significance of polarization is the uncertainty in polarimetric background. The shaded regions around lines in Figure 5 represent the variation of significance for probable variation of the polarimetric background by $\pm20\%$ for the same statistical and systematic errors. It can be seen that, even after considering all these uncertainties, for a 500 mCrab source with 40 % intrinsic polarized fraction,

the polarization can be measured with 3σ confidence with an exposure time of $100 - 150$ ks.

5. Astrophysical significance of CZTI polarimetry

Since polarization measurements with CZTI are possible only for bright (> 500 mCrab) X-ray sources, the obvious candidates are the two eminent sources – Cygnus X-1, a black hole binary and Crab, a pulsar wind nebula. The fact that the initial indication of highly polarized emission from both these sources are available from Integral observations, makes the astrophysical significance of CZTI polarimetric capability more relevant.

For example, in the case of Cygnus X-1, measurements by both IBIS and SPI instruments on INTEGRAL show very high polarization fraction (~65 %) at energies greater then ~250 keV, which is interpreted in terms of the emission from the base of a jet (Laurent et al. 2011) While a significant contribution from the jet to hard X-ray / soft gamma emission has been speculated for some other black hole binaries in literature (Vadawale et al. 2001; Markoff et al. 2001; Vadawale et al. 2003), recent SED modelling of Cygnus X-1 spectral energy distribution by Zdziarski et al. (2014) spanning from radio to MeV range, suggests that significant jet contribution to hard X-ray emission can be achieved only with rather unrealistic parameters. On the other hand there are other models which predict state independent high polarization (Romero et al. 2014; Schnittman & Krolik 2010) as well as moderate polarization only in hard state. Thus the present scenario of polarized nature of hard X-ray emission from Cygnus X-1, both observationally as well as theoretically, is rather confusing and it is important to independently constrain it. In this context we considered various available predictions of X-ray polarization for Cygnus X-1 to investigate whether these can be delineated with CZTI, particularly in the presence of some of the systematic effects such as uncertainty in background, uncertainty in the knowledge of polarization angle etc. (see figure 6).

The possible scenarios considered here (denoted by red, green, black and blue respectively in Figure 6) are − strong polarization signature ($\sim 50\%$) in LHS (low hard state) due
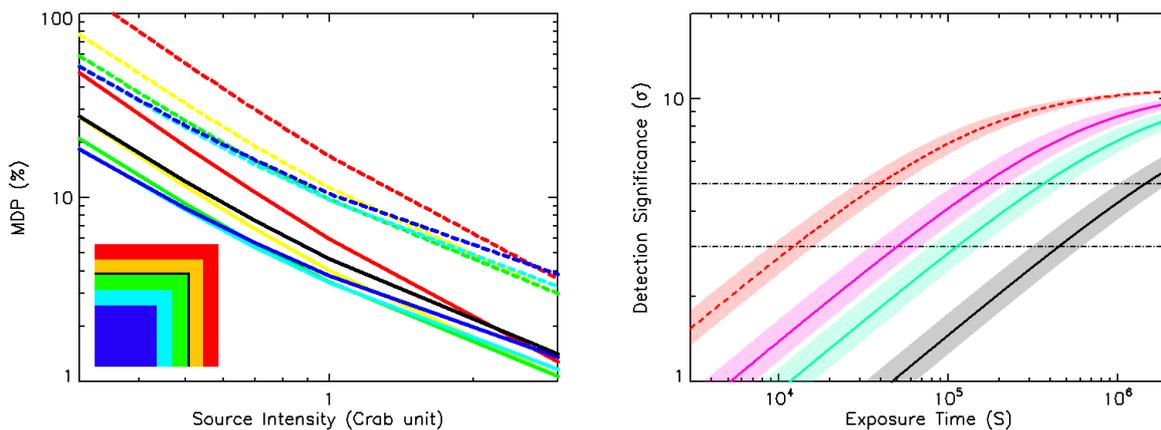
Fig. 5. left: Polarimetric sensitivity of CZTI in terms of MDP as a function of source intensity for exposure time of 1 Ms. The dashed and solid lines represent the polarization angle aligned with the pixel edges and at $45°$ respectively with the latter being more sensitive due to higher modulation factor as expected. Different colors represent sub-samples of CZTI detector plane as shown in the inset. The black line represent the overall MDP as mentioned in the text corresponding to average $22.5°$ polarization and third (green) sub-array. right: Detection Significance of polarization measurement for highly polarized bright sources. The bottom three lines correspond to 500 mCrab sources with polarization fraction of 20% (black), 40% (green), 60% (pink) respectively. The top line (red, dashed) corresponds to 1 Crab source having polarization fraction of 50%.

to relatively high jet contribution; comparatively lower polarization fraction of 25% because of relatively lower jet contribution in LHS; ~15% polarization in LHS originated in corona due to inverse Compton scattering and high polarization (around 55% in high soft state) because of synchrotron radiation from the corona itself. We found that most of the scenarios can be constrained rather accurately within an exposure of time of ~200 ks.

In the case of the Crab nebula, based on the polarization measurements at other wavelengths (including soft X-rays which is the only historic positive X-ray polarization measurement from an astrophysical source (Weisskopf et al. 1978)), it is well known that the nebular emission arises from synchrotron radiation. However, the mechanism as well as the geometry of the emission from the pulsar itself are still not fully understood with various models such as polar cap, outer gap, slot gap, stripped wind (Dyks et al. 2004; Pétri & Kirk 2005), being compatible with all other observational characteristics. One distinguishing feature of these models is their phase-dependent polarization signature. The Integral measurements, folded with the Crab pulse period, suggests that the polarization is varying at different phases, and thus goes against the polar cap model. But in order to constrain other models it is necessary to get truly phase resolved polarization measurements, which typically need an order of magnitude larger exposure time. Since the Crab is likely to be observed for a long duration as a standard candle, it is possible that a total exposure of a few million seconds can be obtained. In such a case, we find that full phase resolved polarization measurement is certainly possible with the lowest polarization also constrained better then 3 sigma. As an example, Figure 6 shows the Crab polarization detection significance, estimated in 16 uniform phase bins. The phase resolved polarization values used in our calculation are obtained by interpolating the recent Crab polarization estimates by IBIS (Moran et al. 2013). Thus we see that CZTI can provide much better insights into the Crab pulsar emission mechanism.

However, polarimetric studies with CZTI will not be limited to only these two sources. There are many transient X-ray binaries, which undergo outbursts lasting from a few weeks to months and have intensities more then 500 mCrab. Since such transient sources are of general interest, it is likely that at least the long outbursts will be observed extensively by Astrosat and thus will result in a total exposure time sufficient for the polarimetric studies with CZTI. Based on the analysis of long term monitoring data from all sky monitors such as RXTE-ASM, SWIFT-BAT and MAXI, we find that typically 2 to 3 outbursts which are brighter then 500 mCrab and longer than one week are expected during the period of one year. Thus, given an operational life of 5 years, CZTI is likely to investigate the presence of highly polarized emission from at least 10 transient sources which are typically black hole and neutron star binaries.

6. Conclusion

To summarize, Astrosat-CZTI will have significant polarimetric capabilities. The polarization capabilities are verified on ground, both with partially polarized beam, and more importantly, with unpolarized beam. This will provide additional confidence to consider the actual polarization measurements as intrinsic to the source and constrain various theoretical models based on them. The GAP (Gamma-ray Burst Polarimeter) instrument, which is a small Compton scattering based polarimeter onboard a Japanese Small Solar Power Sail Demonstrator mission IKAROS (Yonetoku et el. 2011), has demonstrated the importance of robust ground calibration of polarimeters based on which it is successfully measuring polarization of GRBs. The Soft Gamma Ray Detector (SGD), which is a narrow field Compton telescope onboard forthcoming Japanese mission Astro-H (Watanabe et al. 2012) to be launched next year, will also have polarization measurement capability based on Compton scattering principle in 80-300 keV (Tajima et al. 2010). Astrosat-CZTI with much larger area compared to
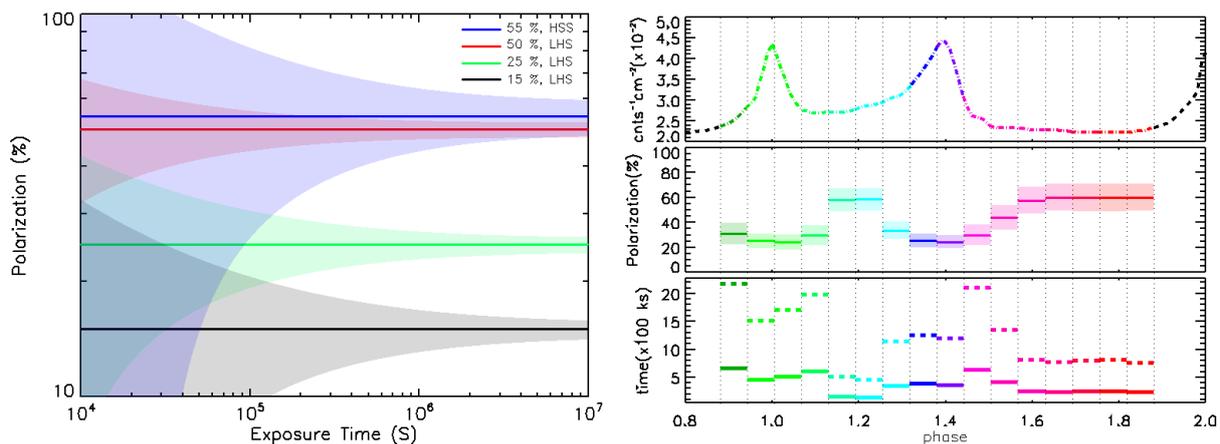
Fig. 6. left: Possible constrains on hard X-ray polarization fraction of Cygnus X-1 for some of the model predictions proposed in literature (see text for details), predicting about 15%, 25% and 50% polarization in low hard state (total flux sin300 mCrab) and about 55% polarization in high soft state (total flux ∼1 crab). Expected errors are shown as shaded regions. right: Feasibility of phase resolved polarimetry with CZTI for Crab. The top panel shows Crab pulse profile in 100 ˇ 300 keV. The middle panel shows polarization in 16 phases as expected from an interpolation of the polarization measured by Integral in four regions of Crab pulse profile. The shaded region represents possible constraints on phase wise polarization measurement with CZTI for a total exposure time of 1 Ms. The bottom panel shows the required exposure time to determine polarization for all phases with a minimum 3 sigma (solid lines) and 5 sigma (dashed lines) confidence levels. It can be seen that with a total exposure time of ∼2 Ms, polarization in most of the phases can be constrained with better then 5 sigma confidence.

GAP and much larger field of view compared to SGD, will prove to be an unique instrument capable of probing the X-ray polarisation of bright celestial sources. Further, Astrosat being an observatory class satellite with X-ray timing as one of its primary objectives, it is likely to devote a large fraction of its observing time to bright X-ray binaries, thus facilitating, as an additional bonus, measurement of X-ray polarisation in the 100 — 300 keV region. Thus it is likely that the field of hard X-ray polarimetry will witness significant advances in the near future.

References

Geant4 Collaboration, Agostinelli, S., Allison, J., Amako, K., et al. 2003, NIMPA, 506, 250ˇ303

Agrawal, P.C. Adv. Space Res. 2006, 38, 2989ˇ2994

Black, J. K., Deines-Jones, P., Hill, J. E., et al. 2010, In Society of Photo-Optical Instrumentation Engineers (SPIE) Conference Series, 7732, id. 77320X, doi:10.1117/12.857736

Chattopadhyay, T., Vadawale, S. V., Rao, A. R., Sreekumar, S., and Bhattacharya, D. 2014, Experimental Astronomy, 37, 555−577.

Coburn, W. and Boggs, S. E. 2003, Nature, 423, 415−417

Costa, E., Bellazzini, R., Tagliaferri, G., et al. 2010, Experimental Astronomy, 28, 137−183

Dyks, J., Harding, A. K., and Rudak, B. 2004, ApJ, 606, 1125−1142

Elsner, R. F., O'Dell, S. L., and Weisskopf, M. C. 2012, In Society of Photo-Optical Instrumentation Engineers (SPIE) Conference Series, 8443. doi:10.1117/12.924889.

Forot, M., Laurent, P., Grenier, I. A., Gouiffès, C., and Lebrun, F. 2008, ApJ, 688, L29−L32

Guo, Q., Beilicke, M., Garson, A., et al. 2013, Astroparticle Physics, 41, 63−72

Dong, Y. 2014, In Society of Photo-Optical Instrumentation Engineers (SPIE) Conference Series, 9144. doi:10.1117/12.2055333

Jahoda, K. 2010, In Society of Photo-Optical Instrumentation Engineers (SPIE) Conference Series, 7732, id. 77320W. doi:10.1117/12.857439

Jourdain, E., Roques, J. P., Chauvin, M., & Clark, D. J. 2012, ApJ, 761, 27

Kallman, T. 2004, Advances in Space Research, 34, 2673−2677

Kislat, F., Beilicke, M., Baring, M.G., et al. 2013 Nuclear Science Symposium and Medical Imaging Conference (NSS/MIC), 2013 IEEE Page(s): 1 - 8. DOI: 10.1109/NSSMIC.2013.6829592

Krawczynski, H., Garson, A., Guo, Q., et al. 2011, Astroparticle Physics, 34, 550

Laurent, P., Rodriguez, J., Wilms, J., et al. 2011, Science, 332, 438

Lei, F.r, Dean, A. J., Hills, G. L. 1997, Space Science Reviews, 82, 309

Markoff, S., Falcke, H., and Fender, R. 2001, A&A, 372, L25−L28

McConnell, M. L., Bancroft, C., Bloser, P. F., et al. 2009, In Society of Photo-Optical Instrumentation Engineers (SPIE) Conference Series, 7435. doi:10.1117/12.826407.

Meszaros, P., Novick, R., Szentgyorgyi, A., Chanan, G. A., and Weisskopf, M. C. 1988, ApJ, 324, 1056−1067

Moran, P., Shearer, A., Gouiffes, C., and Laurent, P. 2013, In An INTEGRAL view of the high-energy sky (the first 10 years) - 9th INTEGRAL Workshop. *ArXiv e-print:*1302.3622.

Novick, R. 1975, Space Science Reviews, 18, 389

Paul, B., Rishin, P. V., Maitra, C., Gopalakrishna, et al. 2010, In Procceddings of The First Year of MAXI: Monitoring Variable X-ray Sources, page 371

Pearce, M., Florén, H.-G., Jackson, M., et al. 2012, Nuclear Science Symposium and Medical Imaging Conference (NSS/MIC), 2012 IEEE, Page(s): 1885 - 1892. DOI: 10.1109/NSSMIC.2012.6551438

Pétri, J. and Kirk, J. G. 2005, ApJ, 627, L37−L40

Romero, G. E., Vieyro, F. L., and Chaty, S. 2014, A&A, 562, L7

Rutledge, R. E. and Fox, D. B. 2004, MNRAS, 350, 1288–1300

Schnittman, J., D., & Krolik, J. H. 2010, ApJ, 712, 908

Singh, K. P., Tandon, S. N., Agrawal, P. C., et al. 2014, In Society of Photo-Optical Instrumentation Engineers (SPIE) Conference Series, 9144, id. 91441S. doi:10.1117/12.2062667.

Soffitta, P., Barcons, X., Bellazzini, R., et al. 2013, Experimental Astronomy, 36, 523−567

Strohmayer, T., E., & Kallman, T., R. 2013, ApJ, 773, 103

Tagliaferri, G., Argan, A., Bellazzini, R., et al. 2010, In Society of Photo-Optical Instrumentation Engineers (SPIE) Conference Series, 7732. doi:10.1117/12.857032.

Tajima, H. et al. 2010, In *X-ray Polarimetry: A New Window in Astrophysics*, Cambridge University Press page 1. *ArXiv e-print:*0905.3708.

Vadawale, S. V., Rao, A. R., and Chakrabarti, S. K. 2001, A&A, 372, 793−802

Vadawale, S. V., Rao, A. R., Naik, S., et al. 2003, ApJ, 597, 1023−1035

Watanabe, S., Tajima, H., Fukazawa, Y. et al. 2012, In Society of Photo-Optical Instrumentation Engineers (SPIE) Conference Series, 8443, id. 844326, doi:10.1117/12.925977.

Weisskopf, M. C. 2010, In *X-ray Polarimetry: A New Window in Astrophysics*, Cambridge University Press page 1. *ArXiv e-print:*0905.3708.

Weisskopf, M.C., Silver, E.H., Kestenbaum, H.L., Long, K.S., & Novick, R. 1978, ApJL, 220, L117

Weisskopf, M.C., Elsner, R.F., & O'Dell, S.L. 2010, in SPIE conf., 7732 *ArXiv e-print:*1006.3711.

Yonetoku, D., Murakami, T., Gunji, S., et al. 2013 PASJ, 63, 625−638

Zdziarski, A. A., Pjanka, P., Sikora, M., and Stawarz, Ł. 2014, MN-RAS, 442, 3243−3255

Weisskopf, M.C., Silver, E.H., Kestenbaum, H.L., Long, K.S., & Novick, R. 1978, ApJL, 220, L117